MULTI-LAYER RADIATION SHIELDING DESIGN FOR COMPACT PROTON THERAPY SYSTEM USING MONTE CARLO SIMULATION

FITROTUN ALIYAH

UNIVERSITI SAINS MALAYSIA

2024

MULTI-LAYER RADIATION SHIELDING DESIGN FOR COMPACT PROTON THERAPY SYSTEM USING MONTE CARLO SIMULATION

by

FITROTUN ALIYAH

Thesis submitted in fulfilment of the requirements
for the degree of
Doctor of Philosophy

September 2024

ACKNOWLEDGEMENT

In the Name of Allah, the Most Gracious and the Most Merciful. Before anything else, I would like to extend my deepest gratitude to Allah, whose assistance enabled me to conclude this doctoral program successfully and punctually. As a result of His benevolence and power, I have acquired numerous conveniences throughout the pursuit of my Ph.D. Alhamdulillah.

I would like to thank my primary supervisor, Dr. Azhar Abdul Rahman, for always supporting, facilitating convenience, and engaging in discussions during this study. I want to express my thanks to my co-supervisor, Dr. Yasmin Md Radzi, for her valuable contributions and insights throughout the research journey. I express my gratitude towards Dr. Imam Kambali, who serves as both the co-supervisor and field supervisor. I appreciate the financial support and access to nuclear facilities provided by the National Research and Innovation Agency (BRIN) Indonesia, which have enabled me to conduct many research activities on using steel slag concrete for radiation shielding.

I also express my thanks to the Ministry of Higher Education Malaysia for financial support of PhD study through the Malaysia International Scholarship (MIS) scholarship. Moreover, this research would not have been possible without financial assistance and facilities from the National Research and Innovation Agency (BRIN) Indonesia, and steel slag aggregate raw materials from PT. Krakatau Posco Indonesia.

Special thanks to Angga Fajar Setiawan, Ph.D, Daffa, Alrivano A, and staffs in Building Materials Laboratory, Civil Engineering Universitas Gadjah Mada, who have assisted in testing steel slag aggregate, making steel slag concrete samples, and testing the characteristics of steel slag concrete. Thanks and appreciation are also extended to

Umar Sahiful Hidayat, M.Eng, and Mahrus Salam, M.Eng. Additional deep appreciation is extended to Argo, Arrijalu, and the staff at the Directorate of Nuclear Facility Management Yogyakarta, whom I cannot mention one by one for their help during experimental data collection. I would also like to thank Darmawati, M.Si, Siti Fatimah Nur Hasanah, S.T for their assistance during the evaluation test of steel slag concrete shielding using the LINAC source at Dr. Sardjito hospital and CT-Scan at UGM hospital.

To my beloved spouse, Ali Mahfud, I extend my gratitude for your support, and continues to assist me in successfully completing this doctoral research. To my dear children, Elton and Meisya, thank you for being great kids. I want to thank my family, who have prayed for and provided moral support while pursuing this PhD study.

TABLE OF CONTENTS

LIST OF TABLES

Page

LIST OF FIGURES

Page

LIST OF SYMBOLS

$\frac{S}{\rho}$	mass stopping power	MeV.cm2/g
dE	Average energy loss	eV
dx	distance	m
ρ	density	g/cm^3
N_A	Avogadro's number	
r_e	electron radius	cm
m_e	mass of an electron	g
c	speed of light	m/s
Z	atomic number	
A	atomic weight	amu
z	charge of the projectile	
β	velocity of the projectile over speed of light	m/s
l	mean excitation potential	
δ	density corrections	
E_p	incident proton energy	MeV
n	neutron	
n_{th}	neutron thermal	
E_n	neutron energy	eV
$\bar{E}_n$	neutron energy average	eV
n_{tot}	neutron total	
ϕ	Fluence	m^{-2}
dN	number of incident particles	

da	cross-sectional area	m^2
D	Absorbed dose	J/kg or Gy
$d\bar{\varepsilon}$	Average energy	J
dm	mass	kg
H_T	Equivalent dose	Sievert (Sv)
R	radiation	
w_R	weight factor (radiation)	
E	Effective dose	Sievert (Sv)
w_T	tissue weighting factor	Sievert (Sv)
H*(d)	Ambient dose equivalent	Sievert (Sv)
H*(10)	Ambient dose equivalent in 10 mm depth	Sievert (Sv)
U	Use factor	
T	Occupancy factor	
θ	angle	°
d	$= d_0/sin(\theta)$, Slant thickness	m
d_0	shielding thickness	m
H_0	source term	Sv m^2
λ	attenuation length	m
g	geometry independent	
r	distance between the target and the point at which the dose equivalent is scored	m
L_i	track length of i-th particle	
W_i	weight of i-th particle	
n_0	total history number	
I	importance	

D_W	dry oven weight	g
SSD_W	surface saturated dry weight	g
$SSD_{W\text{-}in\ water}$	surface saturated dry weight when concrete sample immersed in water	g
σ	modulus of rupture	N/m^2
F	force	N
L	length	m
b	width	m
d	thickness	m
Σ	total macroscopic cross-section	
I_0	Initial radiation intensities	
Σ_ρ	mass attenuation coefficients	
N	Number of protons particle	
Q	electric charge	C

LIST OF ABBREVIATIONS

ACI	American Concrete Institute's
ADS	Accelerator Driven System
ASTM	American Standard Testing and Material
BOF	Basic Oxygen Furnace
BPE	Borated Polyethylene
CPTC	Compact Proton Therapy Center
CPU	Central Processing Unit
CRT	Cathode ray tube
CT-Scan	Computed tomography scan
DCC	Dose Conversion Coefficient
DNA	Deoxyribonucleic acid
EAF	Electric Arc Furnace
EDX	Energy Dispersive X-ray
EGM	Event Generator Mode
ESS	Energy selection system
FFF	Flattening filter free
GEM	Generalized Evaporation Model
GG	General Geometry
HDPE	High-Density Polyethylene
HHS	Health and Human Services
HVL	Half-Value Layer
IAEA	International Atomic Energy Agency
IBA	Ion Beam Applications
ICRP	International Commission on Radiological Protection

ICRU	International Commissions on Radiological Units and Measurements
IF	Induction Furnace
IMPT	Intensity Modulated Proton Therapy
IMRT	Intensity Modulated Radiation Therapy
INC	Intra-Nuclear Cascade
INCL	Intra-Nuclear Cascade Liege
ITZ	Interfacial transition zone
JCPDS	Joint Committee on Powder Diffraction Standard
JQMD	Japan Quantum Molecular Dynamics
LBL	Lawrence Barkeley Laboratory
LET	Linear Energy Transfer
LINAC	Linear accelerator
MCNPX	Monte Carlo N Particle Extended
MeV	Mega electron volt
MHREC	Medical and Health Research Ethics Committee
NCRP	National Council on Radiation Protection and Measurements
NIRS	National Institute for Radiological Science
NRTC	Nuclear Reactor Technology Center
OHRP	Office for Human Research Protections
PC	Portland concrete
PHITS	Particle and Heavy-Ion Transport code System
POI	Point of interest
PPC	Portland Composite Cement
PTCOG	Particle Therapy Cooperative Group
PuBe	Plutonium–Beryllium
QD	Defocusing Quadrupole
QF	Focusing Quadrupole

RBE	Radiobiological effectiveness
REM	Roentgen Equivalent Man
RF	Radiofrequency
UTM	universal testing machine
SEM	Scanning Electron Microscopy
SOBP	Spread-out Bragg Peak
SP	superplasticizer
SSC	Steel slag concrete
SSCA	Steel slag coarse aggregate
SSD	saturated surface dry
SSFA	Steel slag fine aggregate
ST	Sextupole
Vacc	accelerating voltage
WHO	World Health Organization
XRD	X-Ray Diffraction
XRF	X-ray Fluorescence

LIST OF APPENDICES

REKA BENTUK PERISAI SINARAN BERBILANG LAPISAN UNTUK SISTEM TERAPI PROTON PADAT MENGGUNAKAN SIMULASI MONTE CARLO

ABSTRAK

Terapi proton telah muncul sebagai rawatan yang sangat berkesan untuk pelbagai jenis kanser karena ketepatannya dalam menyasarkan sel-sel tumor sambil mengurangkan pendedahan radiasi kepada tisu sihat di sekelilingnya. Walau bagaimanapun, reka bentuk kemudahan terapi proton padat menghadapi cabaran yang besar, terutamanya dari segi keperluan perisai, kos, dan kesan alam sekitar. Kajian ini bertujuan untuk membangunkan reka bentuk perisai baharu untuk sistem terapi proton padat yang mematuhi had dos yang ditetapkan oleh peraturan sambil mengurangkan kos keseluruhan dan keperluan lahan dengan menggunakan bahan alternatif melalui model struktur berlapis. Penyelidikan ini bermula dengan pencirian agregat semula jadi dan sanga keluli sebagai bahan alternatif yang berpotensi untuk campuran konkrit, kemudian diteruskan dengan penilaian eksperimen terhadap sifat pelemahan radiasi menggunakan PuBe, LINAC, dan CT-Scan sebagai sumber radiasi. Untuk mengembangkan dan mengoptimumkan reka bentuk perisai, kajian ini menggunakan simulasi Monte Carlo menggunakan Sistem Kod Pengangkutan Zarah dan Ion Berat (PHITS). Simulasi ini memudahkan penciptaan konfigurasi perisai inovatif, menggabungkan struktur berlapis tunggal dan berbilang lapisan yang terdiri daripada konkrit Portland (PC), konkrit sanga keluli (SSC), besi (Fe), polietilena terborat (BPE), dan Polietilena Ketumpatan Tinggi (HDPE) daripada bahan buangan. Hasil eksperimen menunjukkan bahawa konkrit sanga keluli menawarkan prestasi perisai radiasi yang lebih unggul berbanding konkrit konvensional. Hasil simulasi PHITS

menunjukkan bahawa model kombinasi bahan PC-SSC pada dinding bilik rawatan dan PC-SSC-Fe-HDPE pada dinding Maze 1 adalah konfigurasi yang optimum dengan nilai kadar ambien dos antara 13 hingga 773 mSv/tahun. Ketebalan perisai berlapis pada dinding bilik rawatan proton dapat dikurangkan sehingga 25% – 40% berbanding dengan reka bentuk perisai konvensional yang menggunakan konkrit biasa. Reka bentuk ini bukan sahaja memenuhi piawaian keselamatan peraturan tetapi juga secara signifikan mengurangkan jejak dan kos bahan kemudahan terapi proton sehingga masing-masing 14.2% dan 52%. Penyelidikan ini menyumbang kepada bidang perisai radiasi dan kemudahan perubatan dengan memperkenalkan sanga keluli sebagai bahan yang sesuai untuk sistem terapi proton, disahkan melalui data eksperimen dan simulasi PHITS, serta mempersembahkan penyelesaian reka bentuk yang menjimatkan kos, efisien ruang, dan selaras dengan matlamat kelestarian alam sekitar.

MULTI-LAYER RADIATION SHIELDING DESIGN FOR COMPACT PROTON THERAPY SYSTEM USING MONTE CARLO SIMULATION

ABSTRACT

Proton therapy has emerged as a highly effective treatment for various cancers due to its precision in targeting tumor cells while minimizing radiation exposure to surrounding healthy tissues. However, the design of compact proton therapy facilities poses significant challenges, particularly in terms of shielding requirements, cost, and environmental impact. This study aims to develop a novel shielding design for proton therapy systems that complies with regulatory dose limits while reducing the overall cost and footprint by utilizing alternative materials through a multilayer structure model. The research begins with the characterization of natural aggregate and steel slag as potential alternative materials for concrete admixture, then continues with experimental evaluations of radiation attenuation properties using PuBe, LINAC, and CT-Scan as radiation sources. To further develop and optimize the shielding design, the study employed Monte Carlo simulations using the Particle and Heavy Ion Transport code System (PHITS). These simulations facilitated the creation of innovative shielding configurations, incorporating both single-layer and multilayer structures composed of Portland concrete (PC), steel slag concrete (SSC) , iron (Fe), borated polyethylene (BPE), and recycled high-density polyethylene (HDPE). The experiment results demonstrate that steel slag concrete offers superior radiation shielding performance compared to conventional concrete. The PHITS simulation results demonstrate that the material combination model of PC-SSC on the treatment room wall and PC-SSC-Fe-HDPE on the Maze 1 wall is the optimal configuration with ambient dose equivalent rate value ranging from 13 to 773 mSv/year. The thickness of

the multilayer shielding on the proton treatment room wall can be reduced by up to 25% – 40% compared to the conventional shielding design using ordinary concrete. The design not only meets regulatory safety standards but also significantly reduces the footprint and material costs of proton therapy facilities by up to 14.2% and 52%, respectively. This research contributes to the field of radiation shielding and medical facilities by introducing steel slag as a viable material for proton therapy systems, validated through experimental data and PHITS simulations, and presenting a cost-effective, space-efficient design solution that aligns with environmental sustainability goals.

CHAPTER 1

INTRODUCTION

1.1 Background

Since Robert Wilson proposed to use proton therapy to treat tumors in 1946 the spread out of proton therapy increases significantly (Figure 1.1) (Prusator et al., 2018; PTCOG, 2023). Until April 2021, The Particle Therapy Cooperative Group (PTCOG) noted that there were 98 proton therapy units operated in 20 countries, with the number of proton therapy systems having increased substantially over the past decade. At the end of 2022, more than 300,000 patients have been treated using proton therapy worldwide (PTCOG, 2023).

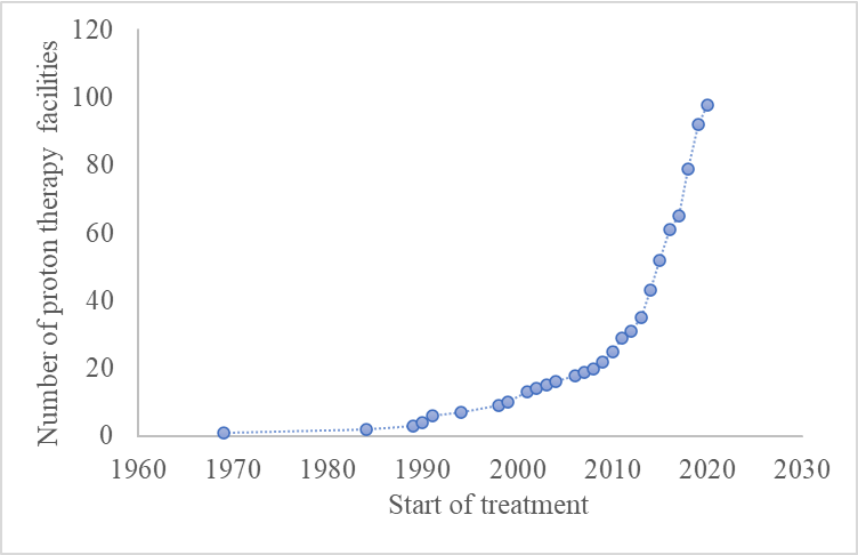

Figure 1.1 Proton therapy facilities growth rate (PTCOG, 2023).

Radiation therapy using high-energy proton radiation technology has developed as an excellent treatment for numerous types of cancer patients (Newhauser and Zhang, 2015). Proton therapy will reduce the amount of radiation exposure to organs at risk. In addition, the amount of radiation beam in treating tumor cells process

is also less compared to the conventional photon therapy. This is due to different dosimetry characteristics of protons as compared with photons used in conventional radiation therapy (Prusator et al., 2018) as shown in Figure 1.2. The maximum energy of proton is near the end of the proton beam range, called the Bragg peak that can be altered according to target volume depth. By varying the proton energy, it will be able to create a dose region that can cover the tumor volume target with high dose accuracy. This area is known as the Spread-out Bragg Peak (SOBP). This technology provides the opportunity for a lower dose in healthy tissue than radiation using photons or X-rays (Alrowaili et al., 2023).

The high energy of proton radiation generates secondary neutron and gamma radiation, which is an important consideration when designing shielding to assure radiation safety (Ardenfors, 2018; Frank, 2021). The shielding wall of the proton therapy system is designed to protect worker and the public from neutron and gamma radiation as well as proton radiation.

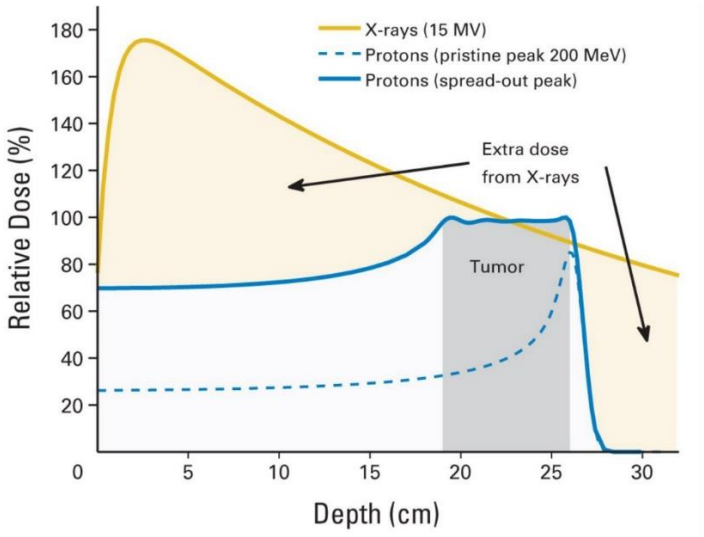

Figure 1.2 Proton and photon depth dose profile (Mitin and Zietman, 2014).

The new facilities of proton therapy are commissioning worldwide every year. Recently, an interest in compact single-room proton therapy systems has grown significantly in the cancer treatment community. It is a cost-effective solution for small hospitals to be involved in proton therapy. The first single-room proton therapy facility supplied by Mevion Medical Systems has shown successful results of operation (Contreras et al., 2016; Mevion, 2021). Based on the Mevion Medical System companies report, developing a compact single-room proton therapy also can reduce high costs, one to ten, compared to a conventional multi-room proton therapy center (Civita and Partnerships, 2019). Currently, most manufacturers propose single-room modifications of supplied equipment. Two of them, i. e. HITACHI and PROTOM developed compact particle therapy systems based on synchrotrons (Vostrikov et al., 2018).

The design of a proton therapy facility with a compact concept requires a more complex shielding compared to the multi-room proton facility. The compact proton therapy system has more limited space with the distance between the radiation source and shielding wall being closer than conventional proton therapy. Those the shielding wall being thicker and higher the neutron activation process with the shielding material. These neutrons activation will produce a radioisotope as nuclear waste (Hennings, 2018).

The conventional shielding design uses Portland concrete as the shielding material. Concrete has several advantages over other materials, including lead, water, rubber, alloy, and others. Firstly, concrete is highly cost-effective, making it a preferred choice in various construction projects. Additionally, concrete possesses the unique ability to be easily moulded to meet the specific design requirements of

buildings. Lastly, concrete demonstrates exceptional structural support capabilities, particularly in the context of nuclear plants. Moreover, concrete has a significant gamma and neutron radiation cross-section. Nevertheless, conventional concrete is deemed unsustainable because of its reliance on natural aggregate obtained through the exploitation of natural resources. Furthermore, its environmental impact is unfavourable because of the substantial release of carbon dioxide (CO_2) emissions. Moreover, traditional concrete necessitates a significant thickness, resulting in an augmentation of both the volume and weight of nuclear devices. Hence, there is a need for the investigation of alternative materials that may serve as a substitute for natural aggregate that is environmentally friendly and possesses favourable characteristics for enhancing the density of concrete, as well as the composition and structure of the material that can be implemented for proton therapy shielding wall to reduce footprint, cost, and environmental damage effect.

Steel slag aggregate, as a byproduct of the steel industry, has the potential value for substituting natural aggregate to produce concrete shielding. The current utilization of steel slag aggregate is limited to specific uses, while the remaining portion is disposed of in landfills. The utilization of steel slag as a concrete addition has witnessed a significant increase in research activities over the past decade, as evidenced by a comprehensive literature analysis (Aliyah et al., 2023). The study on the utilization of steel slag concrete for radiation shielding purposes has mostly focused on gamma radiation, utilizing several radioisotope sources such as Cobalt-60 (Co-60), Cesium-137 (Cs-137), and a moderate neutron energy source represented by Californium-252 (Cf-252). To date, there has been a notable absence of studies undertaken on the utilization of steel slag concrete as a shielding material for proton therapy facilities.

1.2 Problem Statement

Currently, proton therapy is one of the advanced technologies that are in great demand by various countries to reduce the number of cancer sufferers (Civita and Partnerships, 2019; Depuydt, 2018; Garcia-Fernandez et al., 2021; Higgins et al., 2017; Oh, 2019). In addition to reducing radiation exposure to healthy tissue around the tumor, proton therapy also provides a higher chance of survival in post-treatment cancer patients (Arjomandy et al., 2019; Higgins et al., 2017). Therefore, many hospitals or clinics are eager to build a proton therapy system. However, the challenge of shielding design for a proton therapy system because of the high dose of secondary radiation product from proton interaction generated neutron and photon is a crucial consideration. Moreover, the investment and maintenance costs as well as high land requirements are major obstacles for many stakeholders (Civita and Partnerships, 2019; Depuydt, 2018).

The compact single-room proton therapy system with a lower cost and footprint compared to conventional multiroom proton therapy is the best option for hospitals that want to integrate proton therapy with the radiotherapy department. However, the design of a proton therapy facility with a compact concept requires more complex shielding compared to the multi-room proton facility. The compact proton therapy system has more limited space with the distance between the radiation source and shielding wall being closer than conventional proton therapy. The closer the shielding wall, the higher the neutron activation process with the shielding material. These neutron's activation will produce a radioisotope as nuclear waste.

Proton therapy has a byproduct of neutron and photon radiation that contribute to the whole-body dose to patients. The shielding of proton facilities not only protects

patient, worker, and public from proton radiation, but also from neutron and photon radiation. The previous research regarding the material of proton therapy shielding is limited for concrete and iron (Garcia-Fernandez et al., 2021; Lee et al., 2021; Wang et al., 2020). The preliminary study using gadolinium as an admixture material for concrete showed that gadolinium was not effective for high energy neutron shielding due to the characteristic of high cross section for low energy neutron, therefore it should be changed with other materials. There is lack of study regarding the utilization of alternative material derived from waste for shielding of proton therapy facilities which has potential to reduce cost and environmental damage.

Based on previous research regarding the shielding proton therapy design (Garcia-Fernandez et al., 2021; Wang et al., 2020), they reported that single-layer shielding (from concrete or iron material only) requires a larger thickness, of more than 2 meters to 4 meters, to attenuate proton and secondary radiation, which is not appropriate for medical centers with limited area. On the other hand, the multi-layer structure design provides a better shielding effect and significantly lowers the weight of the material (Ma et al., 2018, 2021). In addition, the combination of two materials or more gives the lowest ambient dose rate equivalent behind the shielding (Fragopoulou & Zamani, 2013; Wang et al., 2020). Therefore, the multi-layer design structure using combination of material has the potential to create a thinner shielding and support the development of a compact proton therapy system.

A multi-layer shielding studied by Ma et al. (2021) for an accelerator-driven neutron source show that the combination of Borated Polyethylene (BPE) and lead (Pb) material layers with configuration BPE/Pb/BPE/Pb has been shown to reduce the thickness and weight of the shielding by 60%. Gamma-ray and neutron shielding effect

from multi-layer configuration showed around 10% - 80% better than single-layer structure (Ma et al., 2018). A combination of iron-concrete and iron-BPE with a certain thickness of around 150 cm for shielding of spallation neutron source were the effective material with the lowest ambient dose rate equivalent (Fragopoulou and Zamani, 2013). For proton therapy, the study is still limited to iron and concrete materials (Wang et al., 2020). There is a lack of data in various materials for optimizing multi-layer structure shielding of compact proton therapy.

Neutron shielding is more complex than gamma rays because it must consider the broad spectrum of energy and the neutron characteristics as uncharged particles that can easily pass through the material and interact with atomic nuclei. The incorporation of several materials in a multilayer structure can optimize the shielding's ability to attenuate and absorb neutron radiation. The potential materials to withstand neutron radiation are those with high cross-section values such as high atomic number element, polyethylene, and high content of hydrogen materials.

The investment costs for proton therapy are very high (10× photon therapy) (Medical et al., 2014), with a significant portion of these costs owing to shielding structure. Therefore, the utilization of alternative material from waste can be an attractive option for reducing the cost of raw materials.

This research will design shielding for proton therapy compact systems, especially in treatment room buildings. The shielding currently being developed by the vendor is a single layer using concrete material. The weakness of the one-layer shielding design is that it still requires a relatively high thickness so that the goal of minimizing the footprint of compact proton therapy has not been achieved. To the best of our knowledge, research on the design of multilayer shielding for compact proton

therapy has never been done. The use of a combination of shielding materials consisting of waste resources has also not been reported.

Therefore, this multilayer shielding design using waste products will be one of the novel designs for proton therapy compact systems that have a smaller footprint and costs and are environmentally friendly. This will further pave the way for the development of this multilayer design for standard or commercial purposes.

1.3 Research Objectives

The general objective of the research is to develop a new shielding design for a proton therapy system according to the dose limits set by regulators for individual and environmental safety with lower cost and footprint using alternative materials through a multilayer structure model.

The aims of this work are summarized as follows:

1) To measure the characteristics of natural aggregate and steel slag as an alternative material for the concrete admixture of proton therapy shielding.
2) To evaluate the gamma & neutron attenuation of concrete shielding (as secondary radiation from proton interaction) in different radiation sources using Plutonium Beryllium (PuBe), Linear Accelerator (LINAC), and Computed Tomography CT scan (CT-Scan) as the primary data for validation of proton therapy shielding simulation.
3) To develop the novel design of proton treatment shielding using single-layer and multilayer shielding consisting of Portland concrete (PC),

steel slag concrete (SSC), Fe, BPE, and recycled HDPE through Monte Carlo simulation below the standard of annual dose limit (1 mSv/year).

1.4 Scope and limitation of study

This study's scope consists of four primary elements. The first section describes the raw material characterization that will be used as a concrete shielding material. These materials include natural aggregate (sand and crushed stone) as well as steel slag aggregate. The second step is to create shielding concrete samples with various steel slag aggregate compositions. The steel slag aggregate mixture replaces natural aggregate in the concrete admixture composition at levels of 0%, 20%, 40%, 60%, 80%, and 100%, respectively. The third section examines shielding concrete specimens, which includes density, compressive strength, modulus of rupture, Scanning Electron Microscope (SEM), and radiation testing using neutron and photon sources. The proton source will be employed in the simulation, while the secondary radiation of neutron and photon radiation will be used in the experiment. Plutonium Beryllium (PuBe) is the neutron source, then CT-Scan and LINAC provide the photons. The fourth section simulates and optimizes shielding design using both single and multilayer methods. This section compares conventional shielding designs using a single layer of Portland concrete to single layer shielding from steel slag concrete and multilayer shielding from a combination of Portland concrete, steel slag concrete, borated polyethylene, and high-density polyethylene. The best design will subsequently be evaluated in terms of radiation shielding performance, cost and land requirement analysis. The study is subject to the following limitations:

1. The material utilized is natural aggregate and steel slag aggregate, specifically sand and crushed stone sourced from Yogyakarta, Indonesia,

and steel slag aggregate which derived from the refuse of the steel industry at PT. Krakatau Posco, Indonesia.

2. The materials used for multilayer structures include Portland concrete (PC), steel slag concrete (SSC), iron (Fe), borated polyethylene (BPE), and high-density polyethylene (HDPE).
3. The simulation utilizes proton therapy system with an energy of 230 MeV.
4. The neutron source used in the experiment is PuBe.
5. The photon sources used in the experiment are CT with the head exposure scenario and LINAC with an energy of 10 MV.
6. Shielding design is limited for proton therapy treatment rooms.

1.5 Significance of the Study

The study will contribute to the advancement of proton therapy facility design, the potential for improved safety and cost efficiency in radiation shielding, and an enhanced understanding of steel slag as an innovative shielding material.

1.6 Outline of Thesis

The thesis is structured into five chapters. Chapter 1 commences with providing the background of the study, followed by an overview of the problem statement, research aims, scope and limitation, and the significance of the study. Chapter 2 provides a comprehensive literature review on the history and rationale of proton therapy, the radiological aspects of proton therapy facilities, the compact single-room proton therapy concept, and the challenges and issues in shielding design. Additionally, it explores the use of steel slag material in the shielding concrete and proposes the multilayer concept using Monte Carlo simulation. Chapter 3 outlines the specific research design and approach employed to examine the research objectives. It

contains a concise overview of the study's methodology, including its design, experiment, simulation procedure, and data analysis strategy. Chapter 4 discusses the empirical findings of the investigation. The text examines the data from all aspects of the investigations. The data analysis commences by characterizing the aggregate and shielding concrete. This is followed by assessing the measurement of shielding concrete in various radiation sources. Finally, the analysis concludes with the simulation results of the shielding design for a proton treatment radiation room, considering both single-layer and multilayer structures. Chapter 5 closes the thesis by examining the research findings and offering suggestions for future research to enhance the protective capabilities of steel slag concrete in various energy levels or alternative uses.

CHAPTER 2

LITERATURE REVIEW

2.1 Proton Therapy: History and Rationale

According to the World Health Organization (WHO), cancer is one of the leading causes of death worldwide. Nearly 10 million cancer patients died or 1 in 6 people died in 2018 (WHO, 2021). In 2020, cancer cases in Malaysia reached 48,693 cases with a 5-year prevalence rate of 395.5 (per 100,000 population) (WHO, 2020b). Meanwhile in Indonesia, cancer cases in the same year reached 396,914 cases and the prevalence was slightly lower than in Malaysia at 345.9 (WHO, 2020a).

Most cancer patients receive radiation treatment as a cure. Radiotherapy can be used alone or in combination with other therapies such as chemotherapy or surgery. Through the interaction of atoms and nuclei, radiation can cause mutations or even damage to DNA cells so that they can kill cancer cells. The energy transferred and deposited in the tissue is quantified in "absorbed dose", namely energy per unit mass (Joule/kg) or in units of Gray (Gy) (Paganetti, 2019).

Wilson of Harvard University first proposed the potential use of proton therapy to treat cancer in 1946 who introduced the idea of using finite range and Bragg protons to irradiate tumor targets at certain depths. However, the idea was not immediately developed by the institution where Wilson worked but was taken up by the Lawrence Berkeley Laboratory (LBL), California USA in 1952 (Frank, 2021; Harald Paganetty, 2019; Newhauser and Zhang, 2015). They conducted various experiments, one of which was irradiating mice to study radiobiology. About 30 patients received proton therapy treatment during the period 1954-1957. The technique used is cross-firing, which uses a plateau area on the depth dose curve by performing rotational treatment to

concentrate the dose on the target. While Bragg Peak has not been used (Harald Paganetty, 2019).

The development of the first generation of proton therapy was then followed by the Gustav Werner Institute, Upsala, Sweden in 1955, and the Harvard Cyclotron Laboratory, Cambridge USA in the 1960s. Gustav Werner is the first institution to adopt the SOBP technique as proposed by Wilson using range-modulated to obtain a homogeneous dose plateau in tissue at a certain depth. Meanwhile, the Harvard Cyclotron Laboratory conducted experiments on chromosomal aberrations, death of organisms, and skin tissue reactions to study the radiobiological effectiveness (RBE) of proton beams in tissue which then obtained an RBE value of 1.1 as a conservative value estimate.

The development of proton therapy for the second generation was carried out in Russia and Japan, namely the Joint Institute for Nuclear Research, Dubna, and the National Institute for Radiological Science (NIRS), Chiba. Then followed by several other countries such as Switzerland, UK, France, and South Africa. In this second-generation proton, patients are treated with a broad beam and ridge filter to create a dose distribution plateau (Bragg peak) and begin to be combined with other treatments such as photon and fast neutrons.

The next proton development is hospital-based proton therapy which was first built at Loma Linda University Medical Center California. The development of hospital-based is due to the limited radiation in several centers so the increasing number of patients receiving treatment is quite slow. Loma Linda's proton therapy uses a synchrotron accelerator system. Since then, protons began to be developed commercially with significant improvements.

The rationale for using proton therapy for cancer treatment lies in the aspect of dose distribution (Ardenfors, 2018; Frank, 2021; Hälg and Schneider, 2020; Newhauser and Zhang, 2015). Since proton therapy was first introduced, proton therapy has been able to provide much higher dose conformity to the target tumor than other conventional radiotherapy methods. Although currently, photon therapy is also able to achieve dose conformity according to tumor shape after the discovery of intensity-modulated radiation therapy (IMRT), the integral dose or total dose deposited in body tissues is always much larger than proton therapy, see Figure 2.1 (Frank, 2021; Hälg and Schneider, 2020). In addition, proton therapy still allows for physical improvements to increase the biological effectiveness of proton therapy and achieve a higher therapeutic ratio through scanning beam technology and intensity-modulated proton therapy (IMPT) (Ardenfors, 2018; Frank, 2021; Newhauser and Zhang, 2015).

Although the technology for the use of protons has not been proven and there are still uncertainties about the delivery of the right dose to the tumor target, several recent studies have shown that proton therapy has many advantages over photon therapy. This is supported by a comparative analysis of patients receiving photon versus proton treatment for Non-Small Cell Lung Cancer in 2016. The comparative data show that the survival rate of patients receiving proton therapy is greater than patients receiving photon therapy, which is 22% and 16% respectively (Higgins et al., 2017). Then patients who received proton therapy treatment-experienced far fewer side effects after radiotherapy than patients who received photon treatment (National Cancer Institute, 2020).

The advantages of proton therapy compared to photons are more on the characteristics of proton radiation which has a Bragg peak phenomenon so that by adjusting the beam energy and beam direction, a homogeneous dose can be distributed

over the target tumor volume. Comparison of treatment plans also showed that the total dose received by the patient in the photon treatment was much larger than the proton treatment. For paediatric patients, this is a tremendous advantage because it can reduce the radiation exposure received by the tissue that can cause long-term side effects.

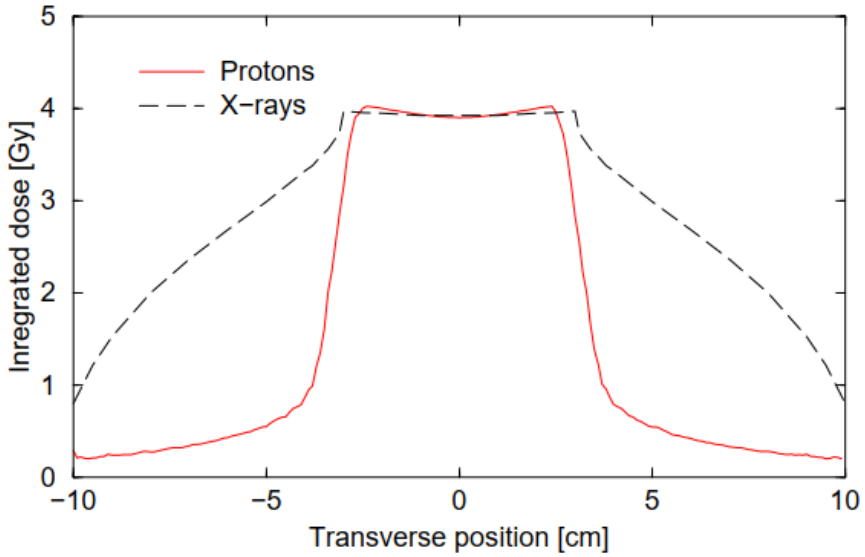

Figure 2.1 Integral dose of proton and X-ray for 6 cm tumor target (Peggs et al., 2002).

2.2 Radiological Aspect of Proton Therapy Facilities

2.2.1 Physics of Proton Interaction Mechanism

Proton interaction with matter occurs in 3 schemes, that is a) Coulomb with atomic electrons, b) Coulomb with an atomic nucleus, and c) nuclear interaction. The three processes have a different percentage chance of events that theoretically can reduce the proton's energy, stop it, and produce secondary products as a result of the interaction (Ardenfors, 2018; Frank, 2021; Harald Paganetty, 2019; Newhauser and Zhang, 2015). The mechanism of proton interactions with matter can be seen in Figure 2.2.

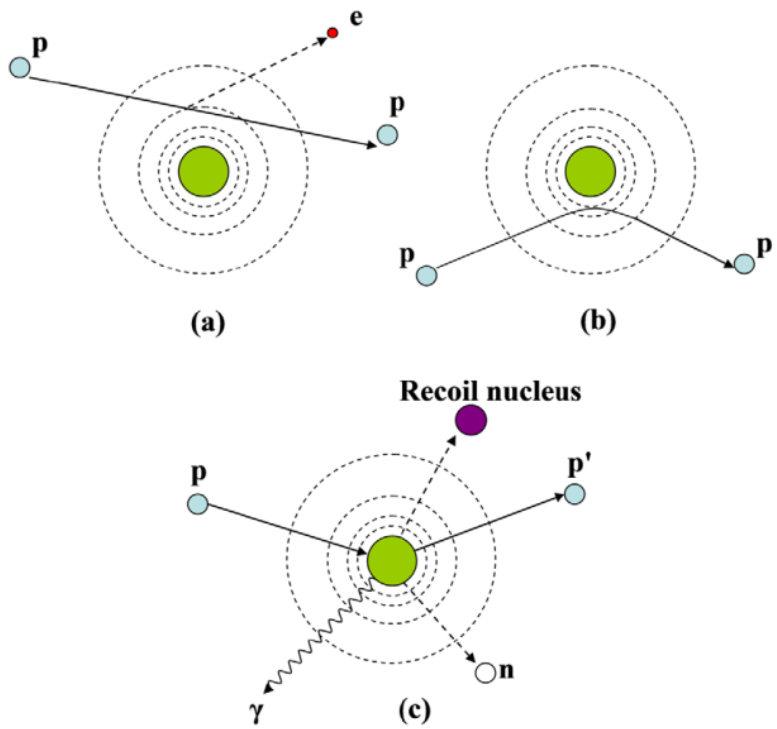

Figure 2.2 Proton interaction with matter (Newhauser and Zhang, 2015).

The coulomb interaction with atomic electrons will cause the proton to lose energy through the process of ionization and atomic excitation and eventually stop by electromagnetic multiples. Because the proton mass is much greater than the atomic electron mass, the direction of the proton remains in a straight line, not deflected. Conversely, when protons approach the atomic nucleus and then interact with the atomic nucleus, inelastic column scattering occurs, causing the protons to be deflected by a large angle. This process contributed to the appearance of the proton beam penumbra. The interaction of protons with the nucleus can also produce inelastic collisions where it causes secondary products as gamma and neutrons. This process is also known as hard scatter. Although the probability is very small, which is about 1%/cm in water or only 20% of proton beams are hard scattering, these interactions have a much superior effect in radiotherapy (Harald Paganetty, 2019).

The proton interaction summary, regarding the type, target, principle ejectiles, influence on projectile, and dosimetry manifestation are described in Table 2.1.

Table 2.1 Proton interaction summary (Newhauser and Zhang, 2015)

Interaction type	Interaction target	Principal ejectiles	Influence on projectile	Dosimetric manifestation
Inelastic Coulomb scattering	Atomic electrons	Primary proton, ionization electrons	Quasi-continuous energy loss	Energy loss determines range in patient
Elastic Coulomb scattering	Atomic nucleus	Primary proton, recoil nucleus	Change in trajectory	Determines lateral penumbral sharpness
Non-elastic nuclear reactions	Atomic nucleus	Secondary protons and heavier ions, neutrons, and gamma rays	Removal of primary proton from beam	Primary fluence, generation of stray neutrons, generation of prompt gammas for *in vivo* interrogation
Bremsstrahlung	Atomic nucleus	Primary proton, Bremsstrahlung photon	Energy loss, change in trajectory	Negligible

As the protons pass through the medium, they are continuously slowed. The energy deposited per unit distance or Linear Energy Transfer (LET) rises until all the energy is reduced and exhausted, then suddenly stops (Frank, 2021). The linear stopping power (S) or energy loss rate is defined as the quotient of the average energy loss (dE) over the density (ρ) and distance (dx) (PTCOG, 2010). For stopping power per mass density of a material $\left(\frac{S}{\rho}\right)$, it is stated in equation 2.1.

$$\frac{S}{\rho} = -\frac{dE}{\rho dx} \tag{2.1}$$

2.2.2 Secondary Radiation Production

For proton accelerators, neutrons dominate the prompt radiation field (Ardenfors, 2018; Hälg and Schneider, 2020). As the proton energy increases, the probability of a nuclear cascade increases because the nuclear reactions threshold is exceeded. At proton energies above 200 MeV, a nuclear cascade process occurs and for energies between 50 – 500 MeV, the neutron yield rises to about E_p^2 where E_p is the incident proton energy (IAEA, 1988).

Neutrons are classified based on their energy which is shown in Table 2.2. When interacting with matter, an elastic or inelastic reaction can occur. Even because they have no charge, neutrons can pass through matter without any interaction. When an inelastic reaction occurs, the atomic nucleus absorbs some of the neutron energy and neutrons can be captured or absorbed by the nucleus through several reactions such as (n,p), (n,2n), (n,α), or (n,γ). For an elastic reaction, the total kinetic energy is constant (PTCOG, 2010).

Table 2.2 Neutron classification

Neutron	*Energy*
Thermal (n_{th})	$E_n \leq 0.5\ eV, \bar{E}_n = 0.025\ eV\ at\ 20°C$
Intermediate	$0.5\ eV\ < E_n \leq 1\ keV$
Fast	$1\ keV\ < E_n \leq 20\ MeV$
Relativistic or high-energy	$E_n > 20\ MeV$

Where E_n is neutron energy and $\bar{E}_n$ is neutron energy average.

Thermal neutrons lose some of their energy through scattering interactions. They spread until they are absorbed by the atomic nucleus and then followed by gamma ray emission, as occurs in neutrons-hydrogen interaction. The gamma ray energy is about 2.22 MeV, and the capture cross-section is 0.33×10^{-24} cm^2. This reaction usually arises in shielding materials of concrete and polyethylene. The borated polyethylene material has the advantage of having a higher cross-section of boron than polyethylene and concrete, which is 3480×10^{-24} cm^2 so that it can capture more thermal neutrons. Moreover, the gamma ray energy of $^{10}B(n_{th},\alpha)^7Li$ is also smaller, around 0.48 MeV (PTCOG, 2010). While neutrons in intermediate energy, they are losing their energy by scattering and absorbed.

Fast energy neutrons undergo elastic and inelastic interactions and then cease to be absorbed by the atomic nucleus. They give up about 7 MeV of energy to become gamma rays during the slow down and absorption process. For neutrons with energies above 10 MeV, the interaction is dominated by inelastic reactions. Meanwhile, neutrons with energies below 10 MeV are dominated by elastic scattering. For neutrons below 1 MeV, the elastic scattering process becomes very important where the neutrons interact with hydrogenous materials like polyethylene and concrete. Therefore, shielding material with high-Z such as steel or iron needs to be coated with hydrogenous material because neutrons that resulted from inelastic reactions have smaller energy below 1 MeV cannot be captured by high-Z materials (steel is transparent to neutrons with an energy of about 0.2 MeV – 0.3 MeV.

While relativistic neutrons are produced from the cascade process in the proton accelerator. These high-energy neutrons are quite significant in spreading the radiation field. Neutrons with energies above 100 MeV, when interacting with shielding materials, will regenerate neutrons into low-energy neutrons and charged particles along with the shielding depth through inelastic interactions.

Proton therapy with energy up to 250 MeV produces complex radiation consisting of charged and uncharged particles like neutrons and gamma. The resulting neutrons (neutron yield) will increase in line with the increase of proton energy. This is following the Agosteo et all research results (Agosteo et al., 2007) which are shown in Table 2.3. Figure 2.3 shows the neutron fluence for 250 MeV proton energy on iron target which was calculated using Monte Carlo simulation Fluka code.

Table 2.3 Neutron yield from proton therapy energy up to 250 MeV using thick iron target (Agosteo et al., 2007)

Proton energy (MeV)	Neutron yield (neutron per proton)			Neutron energy average (MeV)			
	$E_n < 19.6\ MeV$	$E_n > 19.6\ MeV$	n_{tot}	0-10°	40-50°	80-90°	130-140°
100	0.118	0.017	0.135	22.58	12.06	4.96	3.56
150	0.233	0.051	0.284	40.41	17.26	6.29	3.93
200	0.381	0.096	0.477	57.73	22.03	7.38	3.98
250	0.586	0.140	0.726	67.72	22.90	8.09	3.62

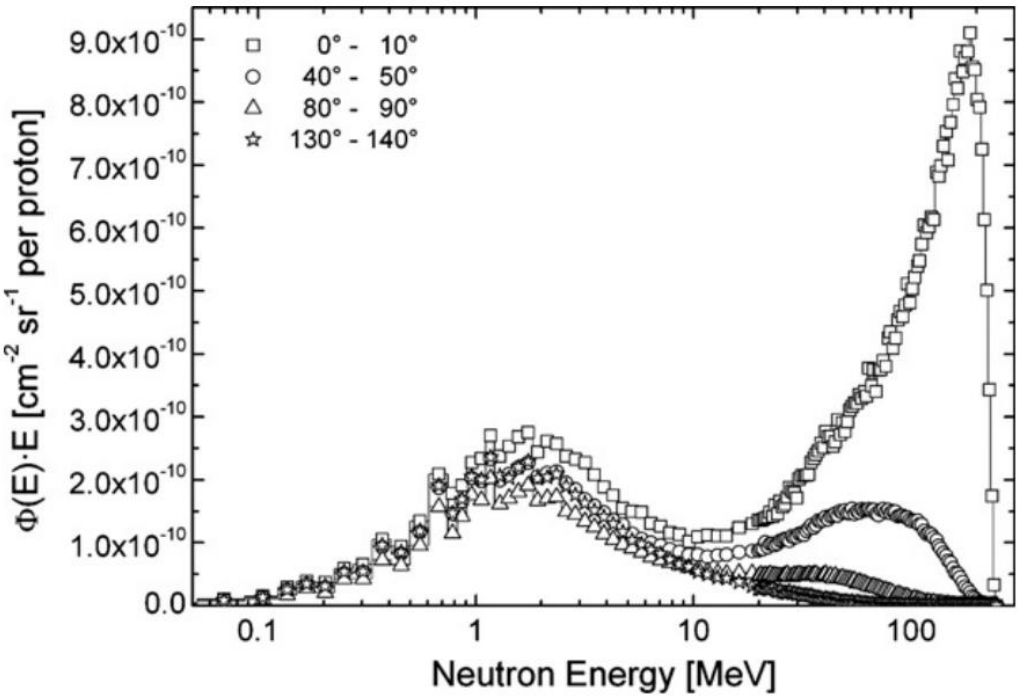

Figure 2.3 Neutron fluence from 250 MeV proton energy on iron target (Agosteo et al., 2007).

2.3 Compact Single Room Proton Therapy Concept

Since proton therapy was first commercialized in the early 1990s, the industry began to develop proton therapy with a compact system. The current trend is to build smaller proton therapy facilities (Garcia-Fernandez et al., 2021). The main goal is to reduce total investment costs in proton therapy projects so that more customers can access them. In comparison, the cost of conventional proton therapy which previously reached more than $100 million can be reduced to less than $50 million or even around

$30 million. Along with the cost impact, the compact system also reduces land for proton therapy facilities (Civita and Partnerships, 2019; Depuydt, 2018; Vostrikov et al., 2018).

Compact proton therapy usually has one or sometimes two treatment rooms, characterized by having advanced equipment to reduce the dimensions and footprint of the facility (Garcia-Fernandez et al., 2021; Owen et al., 2016). Several companies have developed proton therapy with compact designs such as Hitachi, Varian, PROTOM, and Mevion (Civita and Partnerships, 2019; Hitachi, 2021; Mevion, 2021; Protom, 2021; Schillo, 2014; Umezawa et al., 2015; Wang et al., 2020). Conventional multi-room proton therapy and compact single-room proton therapy can be seen in Figure 2.4.

Despite many advantages possessed by a compact proton therapy system, the facility has challenges in terms of shielding design. Space limitation and relatively closer distance between radiation source and patient also shielding wall are important points that need to be considered. The closer the shielding wall, the higher the radiation field, therefore the thicker shielding wall and the higher chance of neutron activation on the shielding material.

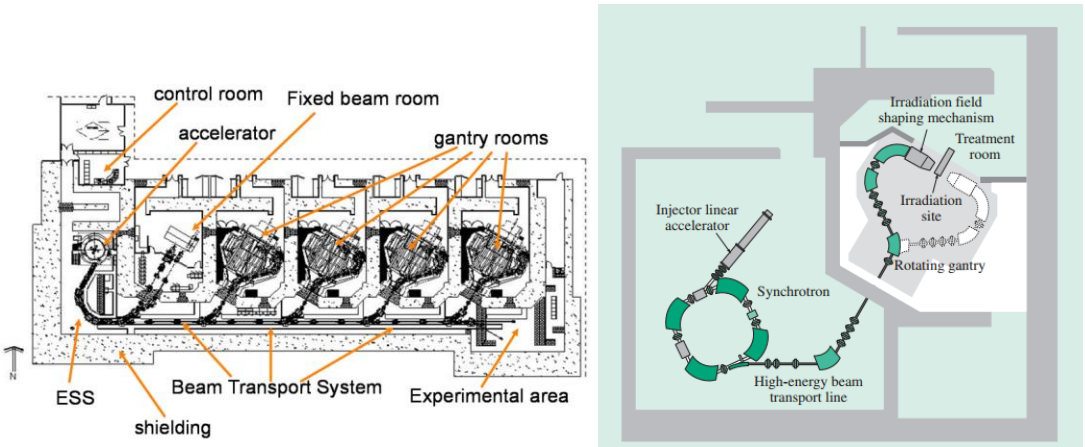

(a) (b)

Figure 2.4 (a) conventional multiroom proton therapy from IBA Proteus®Plus (Kleeven, 2017), (b) compact single-room proton therapy design from Hitachi (Umezawa et al., 2015).

2.4 Radiation Protection Dose Quantities

The impact of ionizing radiation on the human body will have a deterministic and stochastic effect. A deterministic effect occurs when high-dose radiation induces body tissues and causes a detectable symptomatic reaction. Usually, a threshold dose is exceeded before a deterministic effect occurs. While a stochastic is an effect that occurs when low-dose radiation exposes tissues or organs without causing a visible reaction directly. In a long time, stochastic effects can occur such as cell damage, mutation, or cancer. There is no specific dose threshold for this effect (De Smet, 2016; ICRP, 2007).

The calculation of shielding and dose monitoring is merely for radiation protection purposes, specifically by designing facilities to ensure that employees and the public who are exposed to radiation are below the dose limit values set by the International Commission on Radiological Protection (ICRP) or local state regulators. Then the protection quantities value at the dose limit can be measured using proper methods and measurement established by the International Commissions on Radiological Units and Measurements (ICRU) (PTCOG, 2010).

The protection quantities consist of equivalent dose (H_T) and effective dose (E). To understand these protection quantities, it is necessary to know the physical quantities and operational quantities. Fluence, ϕ, is the number of incident particles (dN) in a sphere of cross-sectional area (da). Fluence can be calculated using equation 2.2. The unit of fluence is m^{-2}. The rate of fluence or derivative fluence over time is called flux.

$$\phi = \frac{dN}{da} \tag{2.2}$$

Absorbed dose, D, is the average energy exposed by ionizing radiation to a mass of matter which can be obtained using equation 2.3. The unit for absorbed dose is J/kg, or gray (Gy). The equivalent dose, H_T, is the mean absorbed dose to a tissue T by radiation R with a given weight factor w_R. The equivalent dose, H_T, can be calculated

through equation 2.4. The value of w_R for each type of radiation and energy range has been determined in ICRP publication 103 (ICRP, 2007). The unit of equivalent dose is Sievert (Sv). Then the effective dose, E, is the equivalent dose in tissue or organ T (H_T), times the tissue weighting factor, w_T, see equation 2.5. The unit of effective dose is Sievert (Sv) .

$$D = \frac{d\bar{\varepsilon}}{dm} \quad (2.3)$$

$$H_T = \sum_R w_R D_{T,R} \quad (2.4)$$

$$E = \sum_R w_T H_T \quad (2.5)$$

Ambient dose equivalent, $H^*(d)$, is the dose equivalent value at a point in the radiation field in the ICRU sphere as a theoretical construct of material for tissue-equivalent (diameter of 30 cm, the density of 1 g/cm^3, and mass composition of 76.2% oxygen, 11.1% carbon, 10.1% hydrogen, and 2.6% nitrogen). For strongly penetrating radiation, a depth of 10 mm is recommended, $H^*(d)$.

2.4.1 Conversion coefficient: fluence to ambient dose equivalent H*(10)

The conversion coefficient of fluence to ambient dose equivalent $H^*(10)$ is needed as the basic data for calculating shielding thickness (PTCOG, 2010). If the fluence energy spectrum is known, then the value of operational quantities such as ambient dose equivalent $H^*(d)$ can be calculated using the conversion coefficient relationship. The convention coefficient value is obtained from Monte Carlo simulation for monoenergetic radiation in the reference phantom, both for area monitoring or individual monitoring (De Smet, 2016; ICRU, 1998; Otto, 2019). A schematic of the relationship between the conversion coefficient, operational dose, and protection dose is represented in Figure 2.5. The conversion coefficient value of fluence to ambient dose

equivalent $H^*(d)$ can be obtained from ICRP Publication 74, ICRU Report 57, or Monte Carlo simulation (Figure 2.6 and Figure 2.7).

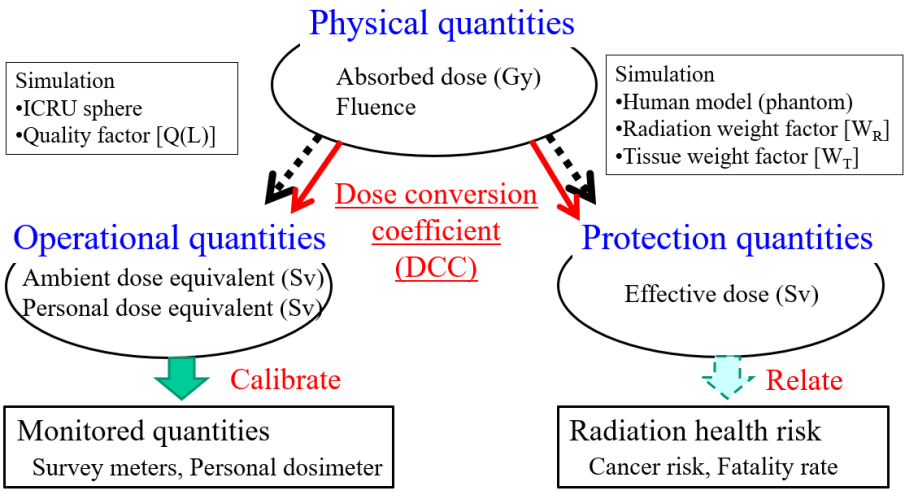

Figure 2.5 conversion coefficient to operational quantities and protection quantities.

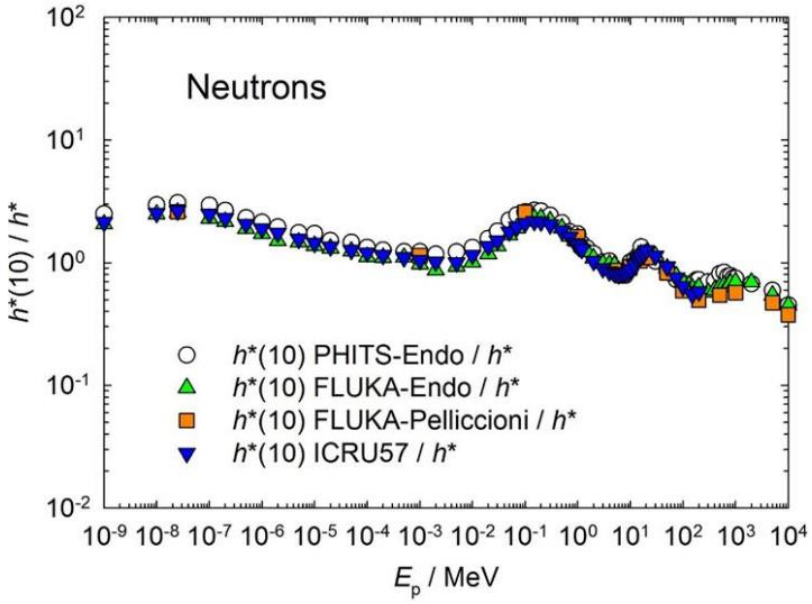

Figure 2.6 Comparison of conversion coefficient of neutron fluence to $H^*(d)$ (Endo, 2017).